

# Potential impacts of Cattaneo–Christov model of heat flux on the flow of Carreau–Yasuda fluid with mixed convection over a vertical stationary flat plate

Amit Kumar Pandey<sup>a</sup>, Sohita Rajput<sup>a</sup>, Krishnendu Bhattacharyya<sup>a,\*</sup>, Ali J. Chamkha<sup>b</sup>, Dhananjay Yadav<sup>c</sup>

<sup>a</sup> Department of Mathematics, Institute of Science, Banaras Hindu University, Varanasi, 221005, Uttar Pradesh, India

<sup>b</sup> Faculty of Engineering, Kuwait College of Science and Technology, Doha District, Kuwait

<sup>c</sup> Department of Mathematical and Physical Sciences, University of Nizwa, Oman

## ARTICLE INFO

### Keywords:

Carreau–Yasuda fluid  
Cattaneo–Christov model of heat flux  
Mixed convection  
Vertical stationary flat plate

## ABSTRACT

Heat transfer in Carreau–Yasuda fluid with mixed convection, effect of Cattaneo–Christov model of heat flux past a vertical flat plate has been studied in this paper. Using appropriate transformations, governing PDEs are reduced to higher order non-linear non-dimensional ODEs and subsequently these are solved using “bvp4c” package of MATLAB. The Carreau–Yasuda fluid is used to explore the behaviour of fluids having shear-thinning and shear-thickening characters for several values of the parameter called power law exponent involved in the fluid model. The effects of different physical parameters, such as Weissenberg number ( $We$ ), thermal relaxation parameter ( $\alpha$ ), Carreau–Yasuda fluid parameter ( $d$ ), mixed convection parameter ( $\lambda$ ) and Prandtl number ( $Pr$ ) on velocity and temperature has been investigated and depicted through graphs. Results reveals that for lower value of  $Pr$  velocity of fluid enhances with higher value of  $\lambda$  and reverse effect is witnessed for larger  $Pr$ . Also, velocity rises for shear-thinning fluid (STNF) and decreases for shear-thickening fluid (STKF) with  $We$  and  $d$ . Temperature exhibits growing behaviour for Cattaneo–Christov model of heat flux near the plate in comparison with Fourier’s model, whereas velocity exhibits growing behaviour with  $\alpha$ . For larger  $We$ , temperature in Carreau–Yasuda model upsurges for STKF and falls for STNF. The surface drag-force displays higher values for both STNF and STKF with growth in  $\lambda$ . The cooling rate rises/declines with  $We$  for STNFs/STKFs.

## 1. Introduction

Heat transfer is one of the significant phenomena of nature through which exchange of thermal energy occurs by dissipating the heat between two systems. It is an important concept which has huge applicability in our everyday lives. The vast subject of heat transfer includes many captivating and critical areas, like steam generators, condensers, and many other heat exchanging equipment in power plants, solar energy conversion for space heating, etc. The scope of heat transfer in industrial applications ranges from simpler steady designs to the advanced one and new-fangled complex operations which produce numerous functions during the production or manufacturing processes. Apart from this, many other industries are using this characteristic in heating and cooling tanks, air-cooled exchangers, nuclear reactor cooling, heat transport in tissue, condenser, condensing boiler and many

more due to possibility of huge transformation power. Fluids are one of the good carriers of heat, as a result, the influence of the fluid’s rheological properties on concurrent diffusion of heat movement is very deep. Several investigations on concurrent heat transmission are addressed in this work. Since most of the fluids being used in the industries are of polymer in nature, the heat transport in fluid with shear-dependant viscosity is essential. For instance, Rehman et al. [1] statistically examined the heat transport in a fluid filled in a channel having grooves containing two circular cylinders heated differentially. Also, Awais et al. [2] statistically investigated heat transmission in Prandtl melting fluid over a cylinder. Abbas et al. [3] investigated impacts of an inclined magnetic field and the distribution of nanoparticles across nonlinearly moving surface. Khan et al. [4] explored magnetic field’s role in energy transport in a fluid on the upper area of paraboloid of revolution. Some other similar works is also available in the literature [5,6]. While Hayat et al. [7]. discussed 3D heat transmission in a flow

\* Corresponding author.

E-mail addresses: [sohita.math@gmail.com](mailto:sohita.math@gmail.com) (S. Rajput), [krish.math@yahoo.com](mailto:krish.math@yahoo.com) (K. Bhattacharyya).

<https://doi.org/10.1016/j.finmec.2023.100179>

Received 12 August 2022; Received in revised form 20 January 2023; Accepted 15 February 2023

Available online 25 February 2023

2666-3597/© 2023 The Authors. Published by Elsevier Ltd. This is an open access article under the CC BY-NC-ND license (<http://creativecommons.org/licenses/by-nc-nd/4.0/>).

Nomenclature		$We$	local Weissenberg number
$C_{fx}$	skin-friction coefficient	$x, y$	Cartesian coordinates ( $m$ )
$c_p$	specific heat capacity ( $JKg^{-1}K^{-1}$ )	<i>Greek symbols</i>	
$D_1$	first Rivlin–Ericksen tensor	$\alpha$	thermal relaxation parameter
$d$	Carreau–Yasuda fluid parameter	$\Gamma$	time constant
$f$	dimensionless stream function	$\eta$	a variable
$Gr_x$	Grasoph number	$\theta$	dimensionless temperature
$Nu_x$	local Nusselt number	$\kappa$	thermal conductivity ( $Wm^{-1}K^{-1}$ )
$n$	power-law exponent	$\lambda$	buoyancy or mixed convection parameter
$Pr$	Prandtl number	$\lambda_1$	relaxation of the heat flux
$q$	heat flux ( $Wm^{-2}$ )	$\mu$	viscosity ( $Kgm^{-1}s^{-1}$ )
$q_w$	surface heat flux ( $Wm^{-2}$ )	$\mu_0$	viscosity with zero shear-rate ( $Kgm^{-1}s^{-1}$ )
$Re_x$	local Reynolds number	$\mu_\infty$	viscosity with infinite shear-rate ( $Kgm^{-1}s^{-1}$ )
$T$	temperature ( $K$ )	$\rho$	density ( $Kgm^{-3}$ )
$T_w$	variable temperature of stationary flat plate ( $K$ )	$\tau$	extra stress tensor ( $Nm^{-2}$ )
$T_\infty$	fixed free-stream temperature ( $K$ )	$\tau_w$	wall shear stress ( $Nm^{-2}$ )
$T_0$	a constant	$\nu$	kinematic viscosity ( $m^2s^{-1}$ )
$u, v$	velocity components ( $ms^{-1}$ )	$\psi$	stream function
$U_\infty$	free-stream velocity ( $ms^{-1}$ )		

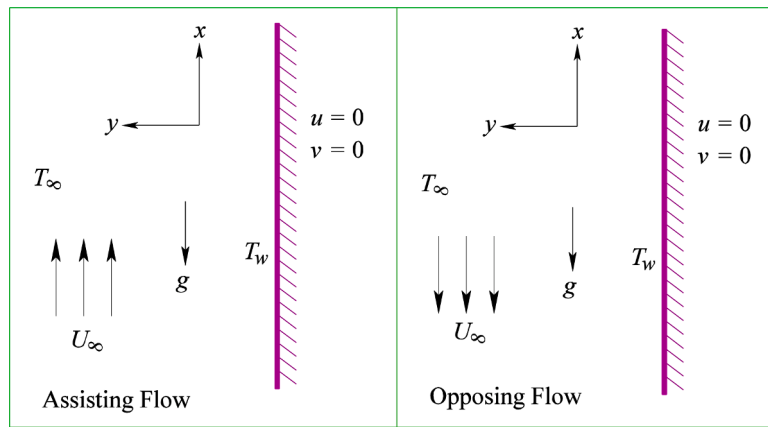


Fig. 1. The physical model of the flow with detailed geometrical structure.

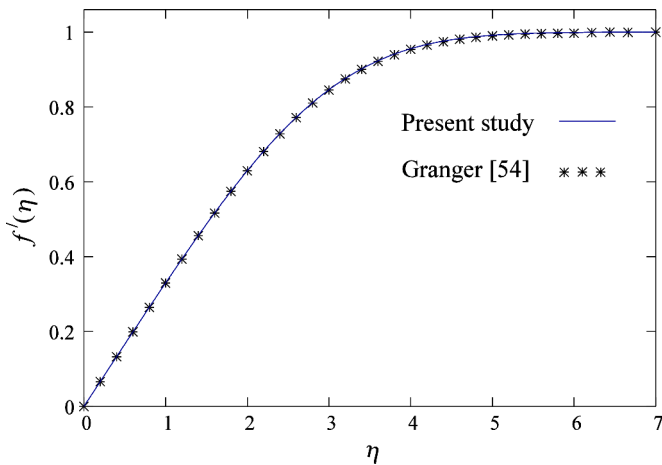
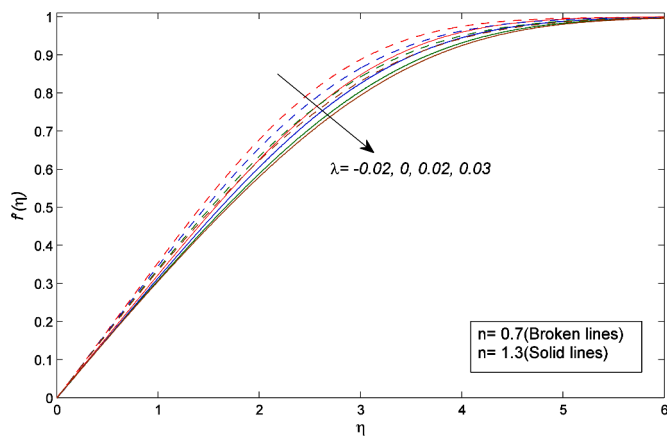


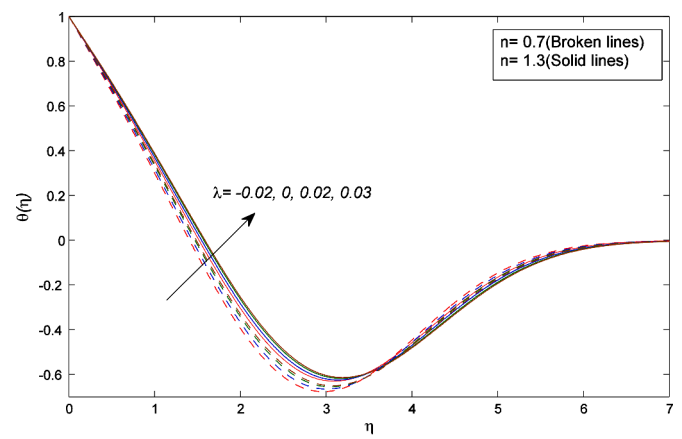
Fig. 2. Comparison of velocity profile for forced convection case and for  $n = 1$  (Newtonian fluid) with the result by Granger[54].

with variable fluid properties on exponentially stretching surface. Sajid et al. [8] inspected flow and heat transmission of a Reiner–Philippoff fluid with nonlinear radiation along an expandable membrane. Sajid et al. [9] also reported impacts of viscous dissipation and non-linear radiation in MHD Carreau fluid flow. The implications of Joule heating, Soret, Dufour, and permeability on the electro-osmotic flow (EOF) with peristaltic motion of an ionic fluid are discussed by Yasmin et al. [10]. Some recent and important advancements in the field of heat transfer were illustrated by Sajid et al. [11] and Salman et al. [12].

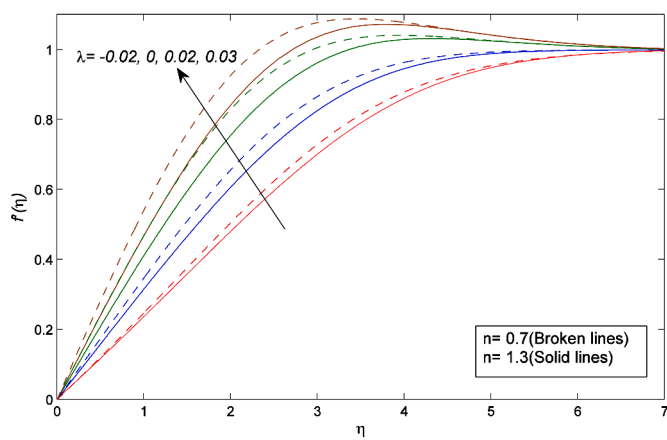
Multiple non-Newtonian rheological constrictive schemes have been proposed based on several properties of polymer fluids showing non-Newtonian behaviour having several usages in industries. Many rheological models, like Carreau liquid [13], Williamson [14], and Carreau–Yasuda [15] models are models with shear rate-dependant viscosity based models. If the shear rate is either low or high, power-law model is unable to forecast viscosity of fluid. Nonetheless, Carreau–Yasuda model is used by scientists and has been extensively used to investigate the influence of shear-thinning character on heat and mass transmission. However, few more relevant works can be explored. The influences of Joule heating and convective boundary conditions on Carreau nanofluid flow across an inclined expanded cylinder with an imposed magnetic field was studied by Khan et al. [16] and underlying



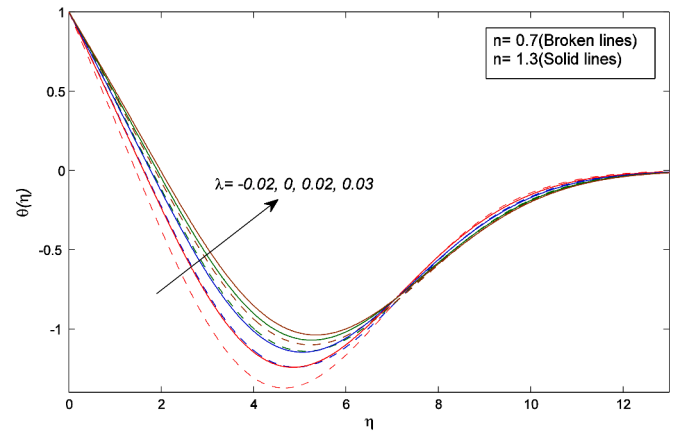
(a)



(a)



(b)



(b)

Fig. 3. Effect of  $\lambda$  on  $f'(\eta)$  when (a)  $Pr = 1$  and (a)  $Pr = 0.2$ .

Fig. 4. Effect of  $\lambda$  on  $\theta(\eta)$  when (a)  $Pr = 1$  and (a)  $Pr = 0.2$ .

equations were solved using numerical approach. The finding of the investigation indicate an inverse relation for shear-thickening fluid (STKF) velocity with higher Weissenberg number, whereas shear-thinning fluid(STNF) velocity is enhanced when substantially large Weissenberg number is assumed. Iqbal et al. [17] compared shear-thickening, Newtonian, and shear-thinning fluids by using different values of material parameters to study Sisko fluid flow that exhibits peristaltic mechanism in an asymmetric channel with sinusoidal wave propagating down its walls. Khan et al. [18] further examined unsteady Carreau nanofluid flow with heat and mass transfer caused by contracting/expanding cylinder with convective heat transfer condition and temperature-dependant conductivity considering thermophoresis and Brownian motion. Khan et al. [19] also employed the bvp4c approach to establish the solution of flow model of Carreau–Yasuda liquid having thermal energy and solutal diffusion involving viscous dissipation on a heated plate. Later, Khan et al. [20]. assessed the impacts of the chemical reaction, viscous dissipation, and heat source on the transfer of heat and species mass over a hot surface, and then they explored the outcomes of flow, temperature fields, and solutal spread versus various parameters. Waqas et al. [21] explored a system of PDEs describing the rheology of Carreau–Yasuda with bio-convection, partial slip, thermal radiation and chemical reaction over expanding surface. Khan et al. [22] investigated flow characteristics related to 2D Carreau–Yasuda flow with contributions of Dufour and Soret effects over a hot surface. Recently, second-grade nanofluid flow and its thermal characters were analysed by Shah et al. [23].

When different temperatures exist, heat transfer occurs between

bodies or between several sections of a body. This behaviour has numerous mechanical and technological implications, such as energy production, cooling electronic equipment, cooling nuclear reactors, electricity generation, and many more [24–26]. Initially, in 1882, Fourier [27] introduced the idea of classical conduction law and since its appearance, this law has served as a foundation for the study of heat transmission mechanisms. The Fourier law for heat conduction reveals a parabolic equation of energy which implies an initial disruption. It is indeed referred to as heat conduction paradox [28] in the literature. In 1948, Cattaneo revised the traditional Fourier law of conduction, by introducing a parameter relaxation time, which allows heat transport processes to be sensitive to thermal wave propagation [29,30]. Following Fourier and Cattaneo, Christov modified the rule further by changing Oldroyd’s upper convected derivative to maintain frame in various generalizations. As a result, the newly developed model is identified as the Cattaneo–Christov model for heat flux, and it can predict the heat transfer characteristics more accurately. Mehmood et al. [31] investigated the Cattaneo–Christov heat flux in a two-dimensional asymmetric channel with non-Newtonian peristaltic flow and identified its non-Newtonian characteristics. On flow due to stretching, Han et al. [32] compared Fourier and Cattaneo–Christov models for heat flux in flow of Maxwell fluid. Hayat et al. [33]. scrutinized homogeneous-heterogeneous reactions and Cattaneo–Christov model for heat flux in a flow near a stagnation-point. El Harfouf et al. [34] reported homotopy perturbation solution squeezing MHD nanofluid flow with Cattaneo–Christov heat flux model. Rasool and Wakif [35] determined influence of Cattaneo–Christov model of heat flux on

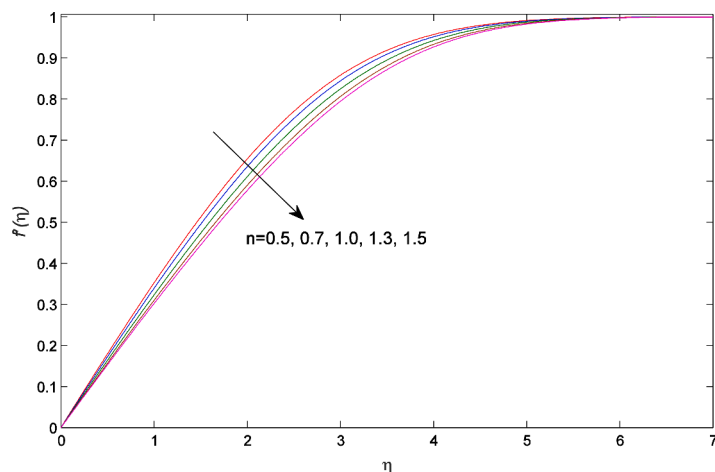


Fig. 5. Effect of  $n$  on  $f'(\eta)$ .

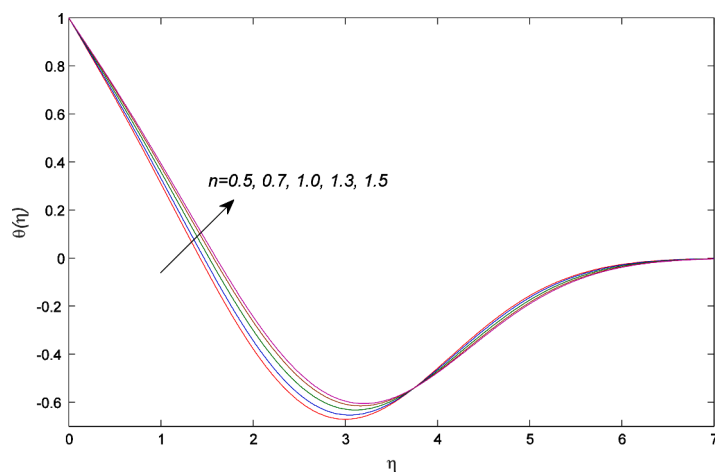


Fig. 6. Effect of  $n$  on  $\theta(\eta)$ .

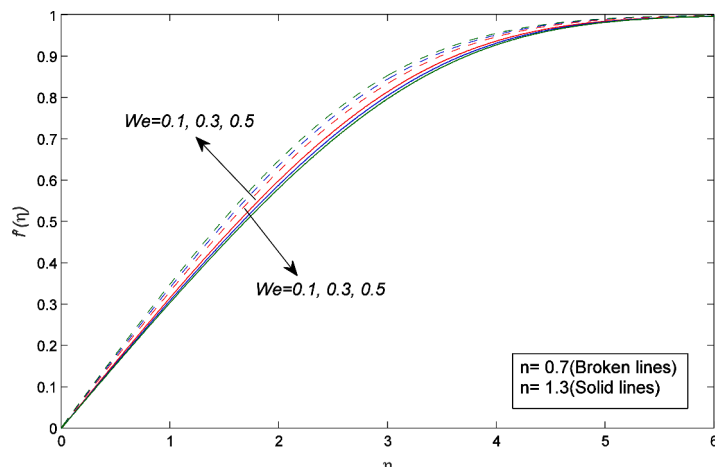


Fig. 7. Effect of  $We$  on  $f'(\eta)$ .

second-grade nanofluid flow over Riga plate. Recently, Abbas et al. [36] discussed the couple stress fluid flow with Cattaneo–Christov model for heat flux.

Mixed convection is generated with joint effort of both forced and free convections. Considerable cases of mixed-convection which are referred to as internal mass forces, in which flow is governed by a few

external sources of force. It occurs in a fluid distribution with varying densities in the gravitational field. Mixed convection is observed in many technical gadgets, but in much smaller scales. The heating/cooling of channel walls, as well as the constrained velocities of fluid flow which are hallmarks of laminar flow, are common examples of mixed convection. The critical uses of this in industries involve things and

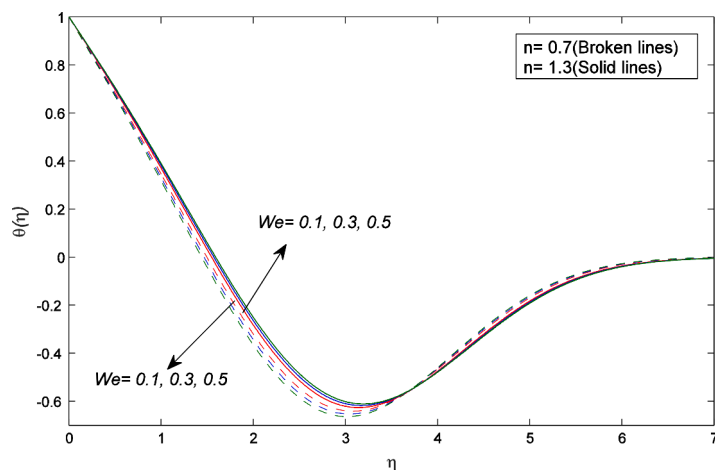


Fig. 8. Effect of  $We$  on  $\theta(\eta)$ .

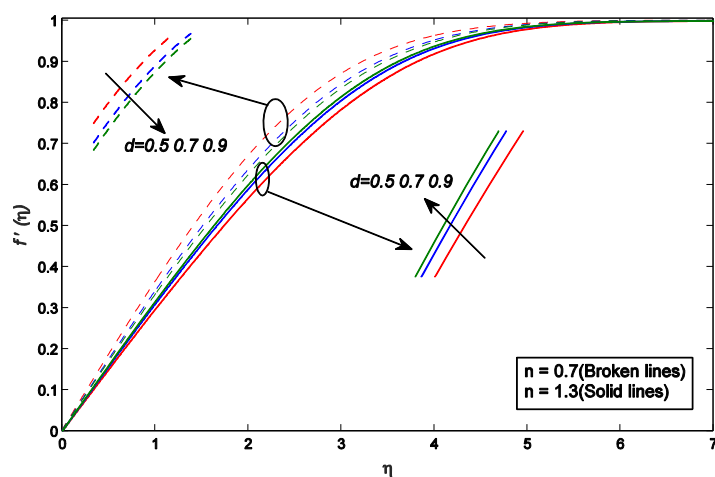


Fig. 9. Effect of  $d$  on  $f'(\eta)$ .

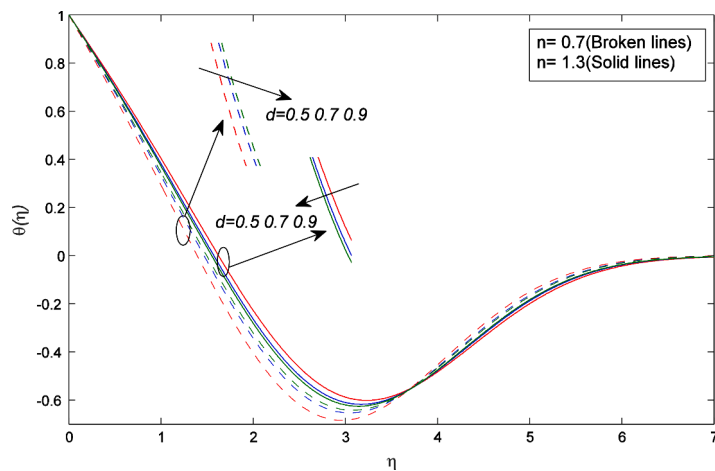


Fig. 10. Effect of  $d$  on  $\theta(\eta)$ .

processes such as electrical gadgets, cooling using electric fans, photovoltaic systems subjected to wind currents, heat transmission in low-velocity situation, flow in ocean and atmosphere, and many more. Mixed convection and its various aspects have been specified by several studies [37–39] in the literature. Gebhart and Pera [40] investigated the natural convection flow created by joint buoyancy effects of

temperature and species along vertical surface. Hussain et al. [41] studied impacts of coupled heat and mass transmission on free convection on vertical plate. Roy and Hossain [42] explained in their research that free convection on fixed vertical plate had the combined influences of sinusoidal variations in wall concentration and temperature. Hayat et al. [43] investigated the peristaltic transport of an incompressible

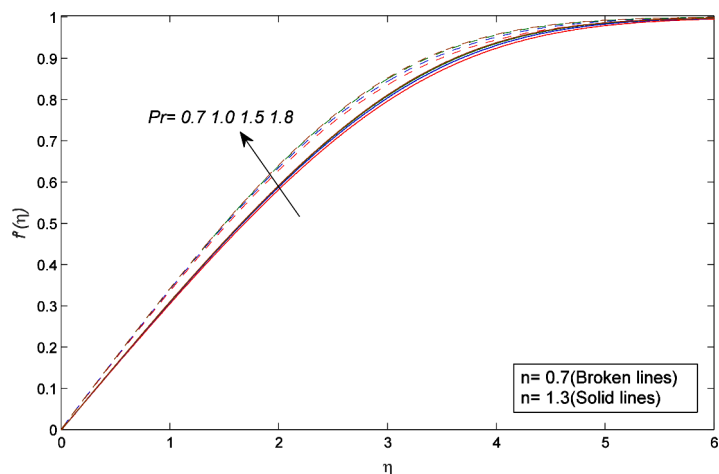


Fig. 11. Effect of Pr on  $f'(\eta)$ .

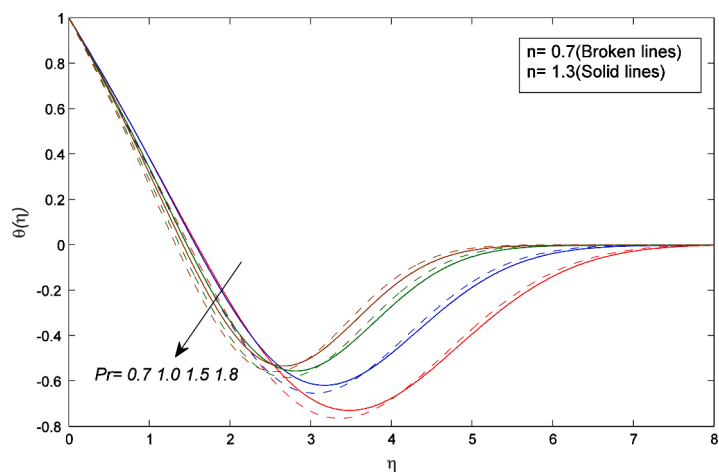


Fig. 12. Effect of Pr on  $\theta(\eta)$ .

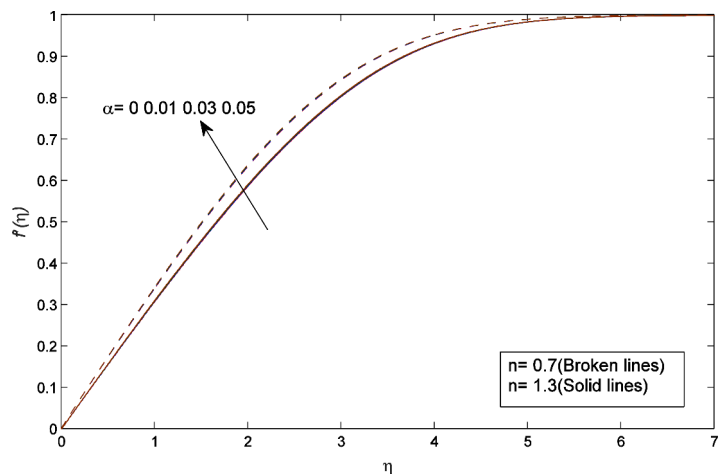


Fig. 13. Effect of  $\alpha$  on  $f'(\eta)$ .

micropolar fluid in an asymmetric channel with heat source/sink and convective boundary conditions and reported solution expressions for stream function, longitudinal velocity, temperature, and pressure gradient. Laminar flow on flat plate with a slip was inspected by Martin and Boyd [44]. The effect of slip on mixed convection on vertical plate was explored by Bhattacharyya et al. [45]. Cao and Baker [46] reported

local non-similar solutions for mixed convection on an isothermal vertical plate taking into account thermal jump and velocity slip. Harris et al. [47] investigated stagnation point flow with mixed convection on vertical surface inside slip-prone porous material. According to Hayat et al. [48] and their discussion of power-law fluid peristaltic flow in an asymmetric channel with convective conditions at the channel walls, a

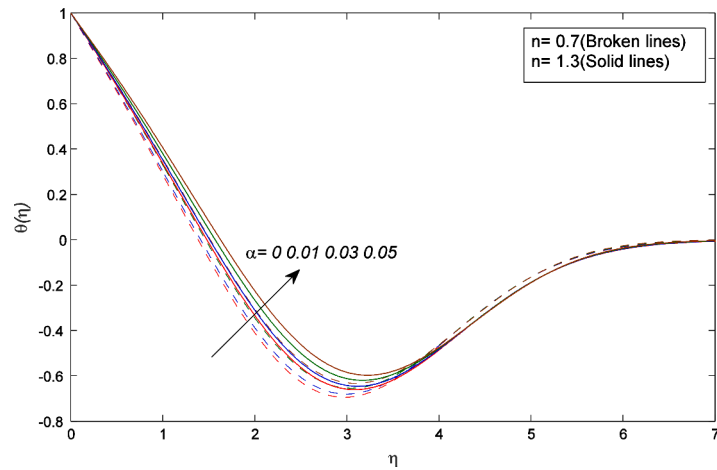


Fig. 14. Effect of  $\alpha$  on  $\theta(\eta)$ .

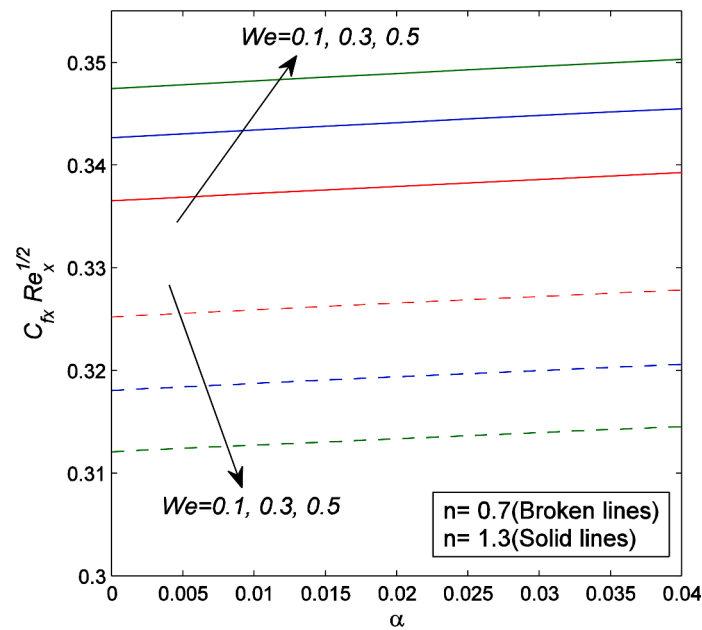


Fig. 15. Influences of  $We$  and  $\alpha$  on skin-friction coefficient.

rise in Biot numbers combined with a power-law fluid parameter produces a fluid temperature decline.

Motivated by non-Newtonian flow behaviour and non-Fourier Cattaneo–Christov model for heat flux and their applications, a mixed convection of Carreau–Yasuda fluid on a flat stationary vertical plate with Cattaneo–Christov heat transfer model is investigated here. The objective of the undertaken investigation is to explore the effect of Cattaneo–Christov model for heat flux in mixed convective flow of Carreau–Yasuda fluid and its heat transfer characteristics to confirm the necessary novelty of the analysis. This investigation may provide an inspiration for future related investigations and their experiments. PDEs those governed the system are converted into ODEs and the solutions are derived using the well-known MATLAB “bvp4c” tool with findings being validated by comparison with previously published work. Additionally, the key consequences depended on governing parameters are described in graphical and tabular modes. Through this study following research questions have been tried to be addressed:

(a) Is there any difference between the effects of Cattaneo–Christov model of heat flux on shear-thinning and shear-thickening fluids ?

(b) What are impacts of buoyancy force on flows two types of fluids in presence Cattaneo–Christov model for heat flux ?

(c) How do the Carreau–Yasuda fluid material parameters affect the heat transfer characteristics for the case of Cattaneo–Christov model ?

The process of getting answers of the above research queries is initiated by the “Mathematical formation” section next. In the Section 3, solutions are obtained and 4th Section is devoted for analysis of results. Lastly, Section 5 states the main findings of the study in the form of concluding remarks.

## 2. Mathematical formulation

In mathematical notation, the extra stress tensor for Carreau–Yasuda non-Newtonian fluid is represented as [19]:

$$\tau = \left[ \mu_{\infty} + (\mu_0 - \mu_{\infty}) \left\{ 1 + (\Gamma \dot{\gamma})^d \right\}^{\frac{n-1}{d}} \right] D_1 \tag{1}$$

Here  $n$ ,  $d$  and  $\Gamma$  represent power-law exponent, Carreau–Yasuda

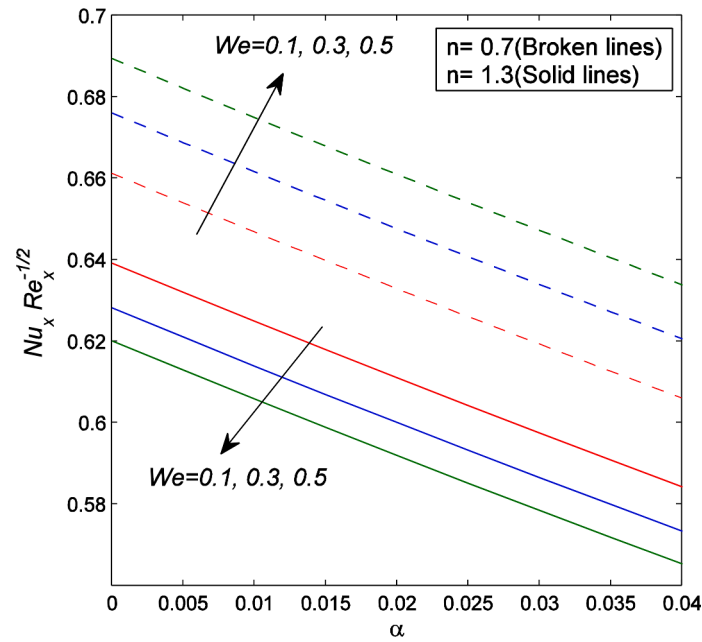


Fig. 16. Influences of  $We$  and  $\alpha$  on Nusselt number.

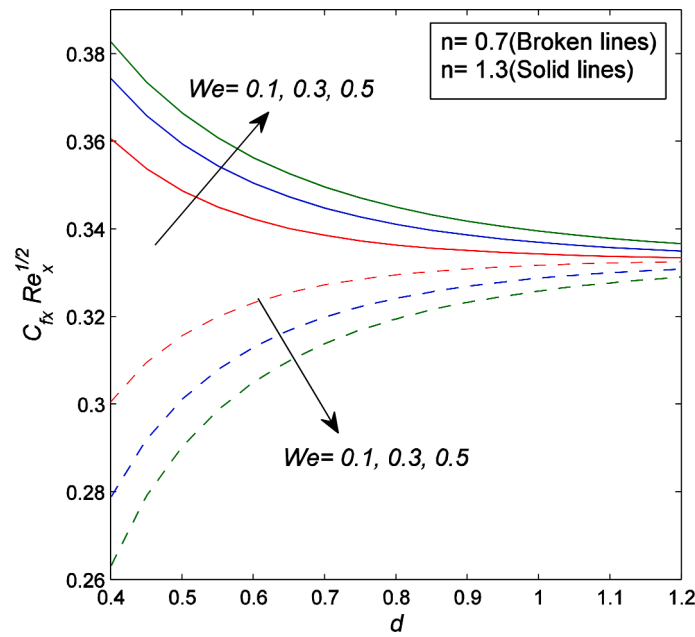


Fig. 17. Influence of  $We$  and  $d$  on skin-friction coefficient.

fluid parameter and time constant, whereas  $\mu_0, \mu_\infty$  indicate viscosities with zero and infinite shear-rates, respectively.

Here  $\gamma$  is represented as:

$$\gamma = \sqrt{2tr(D_1^2)}, \tag{2}$$

where  $D_1$  is referred to as [49]:

$$D_1 = \frac{1}{2} [grad V - (grad V)^T] \tag{3}$$

with  $tr$ ,  $grad$  and  $D_1$  highlight trace, gradient and first Rivlin–Ericksen tensor.

Assuming  $\mu_\infty/\mu_0$  very small, Eq. (1) reduce to

$$\tau = \mu_0 \left[ 1 + (\Gamma\gamma)^d \right]^{\frac{n-1}{d}} D_1. \tag{4}$$

The case of Newtonian fluid is maintained for  $n = 1$ . There are also two distinct instances, namely,  $n < 1$  for shear-thinning fluid(STNF) and  $n > 1$  for shear-thickening fluid(STKF).

To characterize heat transport, Cattaneo–Christov model for heat flow is introduced and which is precribed as [50]:

$$q + \lambda_1 \left[ \frac{\partial q}{\partial t} + V \cdot \nabla q - q \cdot \nabla V + (\nabla \cdot V)q \right] = -\kappa \nabla T, \tag{5}$$

where  $\lambda_1$  is relaxation of the heat flux,  $q$  is heat flux,  $\kappa$  is thermal conductivity. When  $\lambda_1 = 0$ , Eq. (5) reduces to Fourier’s law. By taking into account the incompressibility of fluid, Eq. (5) may be adapted to [50]

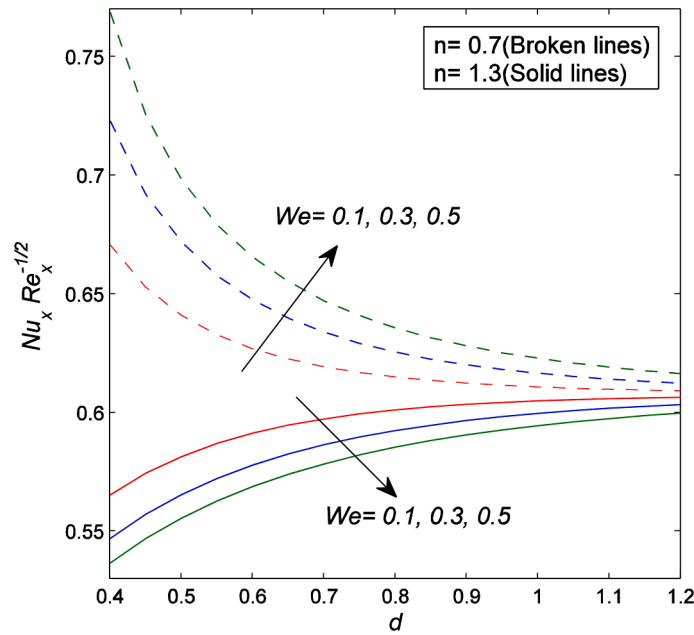


Fig. 18. Influence of  $We$  and  $d$  on Nusselt number.

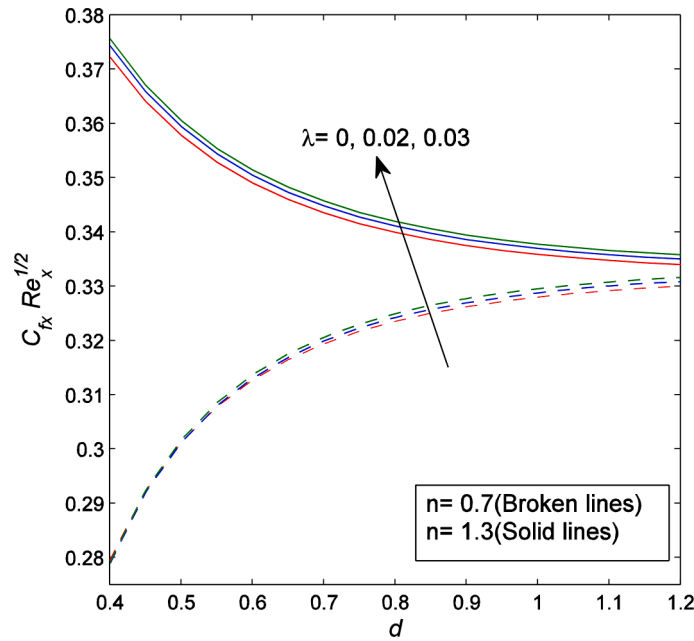


Fig. 19. Influences of  $\lambda$  and  $d$  on skin-friction coefficient.

$$q + \lambda_1 \left( \frac{\partial q}{\partial t} + \mathbf{V} \cdot \nabla q - q \cdot \nabla \mathbf{V} \right) = -\kappa \nabla T. \tag{6}$$

Except density in buoyancy term of momentum conservation equation, all fluid parameters are considered to be constant. The following are the basic equations for mass, momentum, and energy conservations, taking the boundary layer and Boussinesq approximations [50,51]:

$$\frac{\partial u}{\partial x} + \frac{\partial v}{\partial y} = 0, \tag{7}$$

$$u \frac{\partial u}{\partial x} + v \frac{\partial u}{\partial y} = \nu \frac{\partial^2 u}{\partial y^2} + \Gamma^d v \left( \frac{n-1}{d} \right) (d+1) \frac{\partial^2 u}{\partial y^2} \left( \frac{\partial u}{\partial y} \right)^d + g B_T (T - T_\infty), \tag{8}$$

$$u \frac{\partial T}{\partial x} + v \frac{\partial T}{\partial y} + \lambda_1 \left( u \frac{\partial u}{\partial x} \frac{\partial T}{\partial x} + v \frac{\partial v}{\partial y} \frac{\partial T}{\partial y} + u \frac{\partial v}{\partial x} \frac{\partial T}{\partial y} + v \frac{\partial u}{\partial y} \frac{\partial T}{\partial x} \right) + 2uv \frac{\partial^2 T}{\partial x \partial y} + u^2 \frac{\partial^2 T}{\partial x^2} + v^2 \frac{\partial^2 T}{\partial y^2} = \frac{\kappa}{\rho c_p} \frac{\partial^2 T}{\partial y^2}. \tag{9}$$

Note that  $u, v$  indicates velocity components in  $x, y$  Cartesian coordinates.  $T$  is temperature,  $\rho$  is density,  $\nu$  is kinematic viscosity,  $\mu$  is viscosity and  $c_p$  is specific heat capacity.

Boundary conditions for velocity component and temperature are given by

$$u = 0, v = 0 \text{ at } y = 0; u \rightarrow U_\infty \text{ as } y \rightarrow \infty, \tag{10}$$

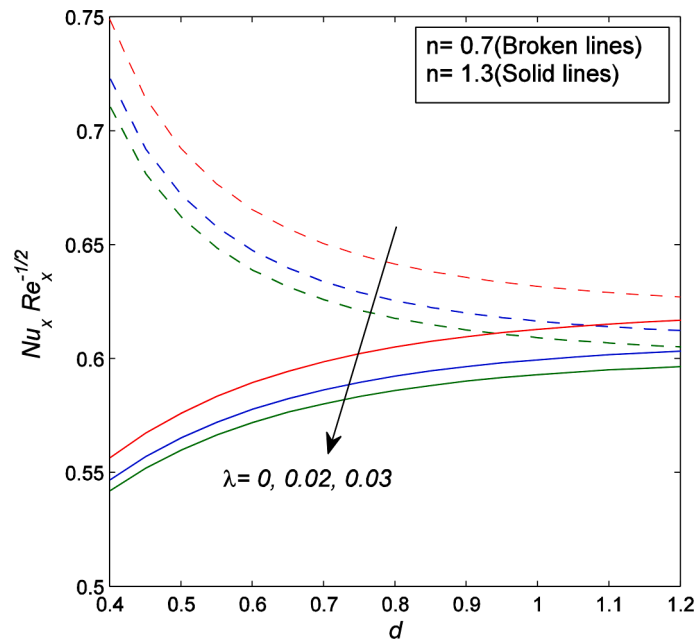


Fig. 20. Influences of  $\lambda$  and  $d$  on Nusselt number.

$$T = T_w, \text{ at } y = 0; T \rightarrow T_\infty \text{ as } y \rightarrow \infty, \tag{11}$$

where  $U_\infty$  is free-stream velocity,  $T_w = T_\infty + T_0/x$  is variable temperature of stationary flat plate with  $T_0$  being a constant representing rate of temperature rise along the surface and  $T_\infty$  describes fixed free-stream temperature. The physical model of the flow with detailed geometrical structure is plotted in Fig. 1.

The following transformations are now implemented as [45]:

$$\psi = \sqrt{U_\infty \nu} x f(\eta), T = T_\infty + (T_w - T_\infty) \theta(\eta), \tag{12}$$

where  $\psi$  being stream function is defined as:  $u = \frac{\partial \psi}{\partial y}$  and  $v = -\frac{\partial \psi}{\partial x}$  with  $\eta$  being a non-dimensional variable. Here  $f$  and  $\theta$  are dimensionless stream function and temperature, respectively.

Through implementation of Eq. (12) we have

$$f'''' \left[ 1 + \left( \frac{n-1}{d} \right) (d+1) f''^{d'} (We^d) \right] + \frac{1}{2} f'''' + \lambda \theta = 0, \tag{13}$$

$$\frac{1}{Pr} \theta'' + \frac{1}{2} f \theta' + f' \theta - \alpha \left\{ \frac{3}{4} f f' \theta' + \frac{1}{2} f'^2 \eta \theta' + \frac{1}{2} f f'' \theta + f'^2 \theta + \frac{1}{4} f^2 \theta'' \right\} = 0 \tag{14}$$

with

$$\left. \begin{aligned} f(0) = 0, f'(0) = 0, f'(\infty) = 1, \\ \theta(0) = 1, \theta(\infty) = 0, \end{aligned} \right\} \tag{15}$$

where  $We = \left( \frac{\Gamma^2 U_\infty^3}{\nu x} \right)^{1/2}$  is local Weissenberg number,  $\lambda = \frac{Gr_x}{Re_x^2}$  is buoyancy or mixed convection parameter,  $Re_x = \frac{U_\infty x}{\nu}$  is local Reynolds number,  $Gr_x = \frac{g \beta (T_w - T_\infty) x^3}{\nu^2}$  is Grashof number,  $\alpha = \frac{\lambda_1 U_\infty^2}{\nu Re_x}$  is thermal relaxation parameter and  $Pr = \frac{\nu}{\alpha} = \frac{\mu c_p}{k}$  is Prandtl number.

The skin-friction coefficient  $C_{fx}$  and local Nusselt number  $Nu_x$  are

$$C_{fx} = \frac{\tau_w}{\rho U_\infty^2} \text{ and } Nu_x = \frac{x q_w}{\kappa (T_w - T_\infty)} \tag{16}$$

where  $q_w$  signifies surface heat flux and  $\tau_w$  denotes wall shear stress for Carreau–Yasuda fluid and those are

$$\tau_w = \left[ \mu \left( 1 + \left( \frac{n-1}{d} \right) \Gamma^d \left( \frac{\partial u}{\partial y} \right)^d \right) \frac{\partial u}{\partial y} \right]_{y=0}, \tag{17}$$

$$q_w = -\kappa \left[ \frac{\partial T}{\partial y} \right]_{y=0}, \tag{18}$$

Following forms of skin-friction and Nusselt number are obtained by employing transformations (12):

$$C_{fx} Re_x^{1/2} = \left[ f''(0) + \left( \frac{n-1}{d} \right) We^d \{ f''(0) \}^d f''(0) \right], \tag{19}$$

$$Nu_x Re_x^{-1/2} = -\theta'(0). \tag{20}$$

### 3. Solution method

The MATLAB function “bvp4c” is used to derive the solution of Eqs. (13) and (14) with (15). Shampine et al. [52] provided the required information on this numerical approach. To follow the approach of the aforementioned method, the first step to solve above equations is to transform those into a set of 1st order ordinary differential equations (ODEs) as presented below:

$$\left. \begin{aligned} y_1' &= y_2, y_2' = y_3, \\ y_3' &= \frac{-\lambda y_4 - \frac{1}{2} y_1 y_3}{\left[ 1 + \left( \frac{n-1}{d} \right) (d+1) y_4^d (We^d) \right]}, \end{aligned} \right\} \tag{21}$$

$$\left. \begin{aligned} y_4' &= y_5, \\ y_5' &= \frac{Pra \left[ \frac{1}{2} y_2 y_2 \eta y_5 + \frac{3}{4} y_1 y_2 y_5 + \frac{1}{2} y_1 y_3 y_4 + y_2 y_2 y_4 \right] - \frac{1}{2} Pr y_1 y_5 - Pr y_2 y_4}{\left[ 1 - \frac{\alpha}{4} Pr y_1 y_1 \right]} \end{aligned} \right\} \tag{22}$$

$$\text{with } y_1(0) = 0, y_2(0) = 0 \text{ and } y_4(0) = 1, \tag{23}$$

$$\text{where } f(\eta) = y_1(\eta) \text{ and } \theta(\eta) = y_4(\eta). \tag{24}$$

The “bvp4c” is a finite-difference algorithm that executes 3-stage Lobatto IIIa collocation formula [53]. Across the integration interval, the collocation polynomial consistently produces a  $C^1$ -continuous solution with fourth-order precision. The error control in the approach is based on residual error, with a level of tolerance of around  $10^{-5}$ . Here, infinity condition,  $\eta \rightarrow \infty$  is approximated to a suitable finite value, say  $\eta_\infty (= 10)$ . Later, for integration of (21)-(24) the appropriate guesses of unspecified initial conditions are supposed to achieve continuous solutions demonstrating the asymptotic convergence to the boundary conditions  $y_2(\eta_\infty) = 1$  and  $y_4(\eta_\infty) = 0$  with aforesaid tolerance  $10^{-5}$ .

### 3. Results and discussion

Computational solutions by aforesaid numerical scheme, “bvp4c” to explore the impacts of various physical parameters involved in the reduced Cattaneo–Christov mixed convection model for Carreau–Yasuda fluid flow have been achieved. To ensure precision level of the applied numerical scheme, the derived result for velocity profile of forced convection case with  $n = 1$  (Newtonian fluid) has been compared with the result of Granger [54] in Fig. 2 and those are found to be in decent agreement, i.e., the results further obtained may be regarded as accurate.

Some selected fixed values of physical parameters are involved, when those are not varying state in the computation and these fixed values are  $\lambda = 0.02$ ,  $Pr = 0.2/1$ ,  $We = 0.3$ ,  $d = 0.7$ ,  $\alpha = 0.03$ ,  $n = 0.7$  and  $1.3$ . However, for demonstrating influence of aforesaid parameters on specific physical property of the flow problem, these parameters are taken to be varied. The impact of various factors is described in this article for two types of values of power-law exponent  $n$ , namely,  $n < 1$  (STNFs) and  $n > 1$  (STKFs). In particular, the values  $n = 0.7$  and  $1.3$  have been taken into account for this study. Fig. 3 depicts the relationship between velocity and  $\lambda$ , which demonstrates that when  $\lambda$  increases, velocity increases for both STNF and STKF, i.e., it rises for aiding flows ( $\lambda > 0$ ) and drops for opposing flows ( $\lambda < 0$ ) for lower value of Prandtl number. The justification behind this findings is that for positive  $\lambda$ , a favourable pressure gradient is generated, which accelerates the motion, whereas for negative  $\lambda$ , the reverse case prevails. It is noteworthy that the buoyancy effect is significantly greater for opposing flows ( $\lambda < 0$ ) than for aiding flows ( $\lambda > 0$ ). The pattern of velocity variations reduces to a completely reverse type for higher Pr values. Fig. 4 depicts the temperature  $\theta(\eta)$  for different thermal buoyancy parameter. For both STNF and STKF, temperature increases with  $\lambda$  for aiding flow and displays a contrary tendency for opposing flow on the plate for any values of Pr. Also, it is showing opposite patterns near and away from the plate and therefore the thickness of thermal boundary layer (TBL) decreases. Furthermore, in forced convection, temperature of fluid is higher in the aiding flow and lower in the opposing flow. The tensor of Carreau–Yasuda model which contains the exponent parameter  $n$ , and its impact on the Carreau–Yasuda fluid flow is investigated (see Fig. 5) and it captures the diminishing phenomena of motion in fluid particles and it is signifies by  $n$ . The numerical value of  $n$  will determine the type of fluid, which are STNF ( $n < 1$ ), Newtonian fluid ( $n = 1$ ), and STKF ( $n > 1$ ). When  $n$  rises to suitably large values, the thickness associated with the boundary layer diminishes. Fig. 6 depicts influence of exponent parameter  $n$  on  $\theta(\eta)$ . When the value of  $n$  increases, the temperature rises near the plate and shows opposing tendencies as it moves away from the plate. Fig. 7 indicates the impact of Weissenberg number ( $We$ ) on  $f'(\eta)$ . Velocity of a STNF increases with  $We$ , while raising the value of Weissenberg number ( $We$ ) results in a decline in viscosity for STKF. Physically, an increase in  $We$  causes higher viscosity, which reduces velocity for STKF. The current approach constructs the Weissenberg number by taking the rheology of the Carreau–Yasuda fluid into account, and  $We$  is defined as a ratio of elastic and viscous forces. Increased relaxation time produces resistance in fluid flow, which is resulting in lower velocity with increased  $We$  for STKF and contrary nature is witnessed for STNF.

Also, the effect of changing dynamic viscosity as a function of shear-rate is identified by the change of  $We$ . The temperature variation with  $We$  is depicted in Fig. 8, which demonstrates that the temperature has a growing trend when ( $We$ ) increases for STKF and reduces for STNF near the plate, but it exhibits reverse behaviour when moving away from the plate. Fig. 9 demonstrates the change in velocity as a function of  $d$ . During the flow, resisting force is generated for large values of  $d$ . So, in STKF, the velocity of fluid particles decreases as  $d$  increases and MBL is a diminishing function of  $d$ . Whereas, contrasting pattern exhibits in shear-thinning fluid. Fig. 10 illustrates the influence of  $d$  on  $\theta(\eta)$ . In this scenario, raising values of  $d$  causes the rise of temperature near the plate for STNF, while temperature falls near the plate for STKF. Furthermore, moving away from the plate, the results exhibit opposite behaviour for both type of fluids (STNF and STKF). For mixed convection, Prandtl number  $Pr$  has influences on velocity field as well as temperature distribution. Fig. 11 depicts the effect of  $Pr$  on  $f'(\eta)$ , with increasing  $Pr$  values for both instances, i.e., for STNF and STKF, velocity exhibits increasing trend. Fig. 12 illustrates impact of  $Pr$  on temperature, which shows a significant reduction in temperature with  $Pr$  for STNF ( $n < 1$ ) and STKF ( $n > 1$ ) near the plate, which is indisputable because a higher Prandtl number correlates to low thermal diffusivity. Momentum diffusivity to thermal diffusivity ratio is expressed by the  $Pr$ . So,  $Pr$  can be employed to increase rate of cooling in a conducting flow. Influence of thermal relaxation parameters  $\alpha$  on  $f'(\eta)$  is shown in Fig. 13. The velocity for STNF/STKF increases with value of  $\alpha$ . Fig. 14 depicts influence of  $\alpha$  on  $\theta(\eta)$ . When value of  $\alpha$  grows, the temperature for STNF/STKF near the plate increases. Furthermore, for both STNF and STKF, lower fluid temperature away from the plate is witnessed with greater values of  $\alpha$ . The physical argument behind the outcome may be stated as with increasing the  $\alpha$ , particles of fluid material require longer time to transmit energy to their nearby particles and consequently, increasing the value of the  $\alpha$  produces a drop in temperature.

Fig. 15 depicts effects of  $\alpha$  and  $We$  for two values of  $n$  on skin-friction related to wall drag force. When  $We$  ( $= 0.1, 0.3, 0.5$ ) rises, skin-friction increases for STKF and reduces for STNF. Also, for increasing thermal relaxation parameter  $\alpha$ , surface drag increases for both STNF and STKF. The effects of  $\alpha$  on the local Nusselt number, i.e., surface cooling rate for various values of Weissenberg number  $We$  are displayed in Fig. 16. On increasing thermal relaxation parameter  $\alpha$ , the heat transfer rate declines for both STNF and STKF. Nusselt number growths for STNFs and reduces for STKFs as value of  $We$  increases. It is also worthnoting that skin-friction and Nusselt number results are prominent for STNFs than those are for STKFs. Fig. 17 demonstrates the effects of  $d$  on skin-friction via  $We$  and  $n$ . It displays that on increasing  $d$  the skin-friction rises for STNF, while it falls for STKF. For several values of Weissenberg number ( $We$ ), Fig. 18 represents effect of Carreau–Yasuda parameter  $d$  on local Nusselt number. With rising values of  $We$ , the Nusselt number for STNF increases, while it decreases for STKF. Also, heat transfer rate increases for STKF and shows opposite trends for STNF, as the value of  $d$  grows. The effects of  $\lambda$  and  $d$  on skin-friction coefficient are displayed in Fig. 19. Skin-friction increases for both STNF and STKF with  $\lambda$ . Fig. 20 portrays effects of  $\lambda$  and  $n$  on Nusselt number with  $d$ . When value of  $\lambda$  rises, the cooling rates for both STNF and STKF reduce.

### 4. Conclusions

Present study aims to examine the Cattaneo–Christov model for heat flux on non-Newtonian Carreau–Yasuda fluid mixed convective flow across a vertical flat plate. To solve the final transformed ODEs, the MATLAB package “bvp4c” is employed. The key outcomes of investigation can be summarized as follows:

- When the Weissenberg number is large, temperature of Carreau–Yasuda model rises for STKF and decreases for STNF.

- As Weissenberg number,  $We$  and Carreau–Yasuda parameter,  $d$  rise, velocity rises for STNF and falls for STKF.
- Temperature shows growing behaviour of Cattaneo–Christov model for heat flux near the plate in comparison with Fourier’s law. Also, velocity displays growing behaviour.
- For large values of power-law exponent  $n$ , velocity exhibits a decreasing trend and temperature shows opposite nature.
- The velocity upsurges, while temperature drops with mixed convection parameter.
- Higher Prandtl number causes increment of velocity and decrement of temperature near the plate, but has the reverse effect far away from it.
- For STNFs, the local Nusselt number rises with  $We$ , whereas for STKFs, the contrary trend is observed, Whereas  $We$  has the opposite influence on skin-friction coefficient.
- The skin-friction increases for both STNF and STKF with growing values of  $\lambda$ .

At last, it can be concluded that this investigation has explored the variations in thermal boundary layer for Cattaneo–Christov model of heat flux on Carreau–Yasuda fluid convection across a vertical flat plate. Also, this study has revealed the various control points of involved parameters which help in achieving high cooling rate and hence it makes it highly relevant from application viewpoints.

The time dependant flow case of this problem should be considered as future research. Also, if the flow medium is changed to a porous medium then the new problem may give a better alternative for a rapid heat transfer process and so the same problem in presence porous medium will be very interesting to be explored.

### Declaration of Competing Interest

The authors declare that they have no known competing financial interests or personal relationships that could have appeared to influence the work reported in this paper.

### Data availability

No data was used for the research described in the article.

### Acknowledgements

The works of A.K. Pandey [09/013(0742)/2018-EMR-I] and S. Rajput[09/013(0843)/2018-EMR-I] are funded by CSIR. Authors are grateful to the anonymous reviewers for their helpful comments and suggestions.

### References

- [1] K.U. Rehman, Q.M. Al-Mdallal, A. Qaiser, M.Y. Malik, M.N. Ahmed, Finite element examination of hydrodynamic forces in grooved channel having two partially heated circular cylinders, case study, *Therm. Eng.* 18 (2020), 100600, <https://doi.org/10.1016/j.csite.2020.100600>.
- [2] M. Awais, S. Bilal, K.U. Rehman, M.Y. Malik, Numerical investigation of MHD Prandtl melted fluid flow towards a cylindrical surface: comprehensive outcomes, *Can. J. Phys.* 98 (2020) 223–232, <https://doi.org/10.1139/cjp-2018-0582>.
- [3] N. Abbas, S. Nadeem, A. Saleem, M.Y. Malik, A. Issakhov, F.M. Alharabi, Models base study of inclined MHD of hybrid nanofluid flow over nonlinear stretching cylinder, *Chin. J. Phys.* 69 (2020) 109–117, <https://doi.org/10.1016/j.cjph.2020.11.019>.
- [4] M. Khan, T. Salahuddin, M.Y. Malik, M.S. Alqarni, A.M. Alqahtani, Numerical modeling and analysis of bioconvection on MHD flow due to an upper paraboloid surface of revolution, *Phys. A: Stat. Mech. Appl.* 553 (2020), 124231, <https://doi.org/10.1016/j.physa.2020.124231>.
- [5] S. Bilal, S. Muhammad, A. Tassaddiq, A.H. Majeed, K.S. Nisar, F. Ali, M.Y. Malik, Computational and physical examination about the aspects of fluid flow between two coaxially rotated disks by capitalizing non-Fourier heat flux theory: finite difference approach, *Front. Phys.* 7 (2019) 209, <https://doi.org/10.3389/fphy.2019.00209>.
- [6] M.S. Sadeghi, N. Anadalibkha, R. Ghasemiasl, T. Armaghani, A.S. Dogonchi, A. J. Chamkha, H. Ali, A. Asadi, On the natural convection of nanofluids in diverse shapes of enclosures: an exhaustive review, *J. Therm. Anal. Calorim.* 147 (2020) 1–22, <https://doi.org/10.1007/s10973-020-10222-y>.
- [7] T. Hayat, M.I. Khan, M. Farooq, N. Gull, A. Alsaedi, Unsteady three-dimensional mixed convection flow with variable viscosity and thermal conductivity, *J. Mol. Liq.* 223 (2016) 1297–1310, <https://doi.org/10.1016/j.molliq.2016.09.069>.
- [8] T. Sajid, M. Sagheer, S. Hussain, Impact of temperature-dependent heat source/sink and variable species diffusivity on radiative Reiner–Phillippoff fluid, *Math. Probl. Eng.* 2020 (2020), 9701860, <https://doi.org/10.1155/2020/9701860>.
- [9] T. Sajid, M. Sagheer, S. Hussain, Role of Maxwell velocity and smoluchowski temperature jump slip boundary conditions to non-Newtonian Carreau fluid, *Front. Heat Mass Transf.* 14 (2020) 28, <https://doi.org/10.5098/hmt.14.2>.
- [10] H. Yasmin, N. Iqbal, Convective mass/heat analysis of an electroosmotic peristaltic flow of ionic liquid in a symmetric porous microchannel with Soret and Dufour, *Math. Probl. Eng.* 2638647 (2021) 1–14, <https://doi.org/10.1155/2021/2638647>.
- [11] T. Sajid, M. Sagheer, S. Hussain, F. Shahzad, Impact of double-diffusive convection and motile gyrotactic microorganisms on magnetohydrodynamics bioconvection tangent hyperbolic nanofluid, *Open Phys.* 18 (1) (2020) 74–88, <https://doi.org/10.1515/phys-2020-0009>.
- [12] S. Salman, M. Qasim, A. Alderremy, S. Noreen, Heat transfer enhancement using different shapes of Cu nanoparticles in the flow of water based nanofluid, *Phys. Scr.* 95 (5) (2020), 055209, <https://doi.org/10.1088/1402-4896/ab4ff4>.
- [13] P.J. Carreau, Rheological equations from molecular network theories, *Trans. Soc. Rheol.* 16 (1972) 99–127, <https://doi.org/10.1122/1.549276>.
- [14] R.V. Williamson, The flow of pseudoplastic materials, *Ind. Eng. Chem.* 21 (11) (1929) 1108–1111, <https://doi.org/10.1021/ie50239a035>.
- [15] K.Y. Yasuda, R.C. Armstrong, R.E. Cohen, Shear flow properties of concentrated solutions of linear and star branched polystyrenes, *Rheol. Acta* 20 (1981) 163–178, <https://doi.org/10.1007/BF01513059>.
- [16] I. Khan, M.Y. Malik Shafquatullah, A. Hussain, M. Khan, Magnetohydrodynamics Carreau nanofluid flow over an inclined convective heated stretching cylinder with Joule heating, *Results Phys* 7 (2017) 4001–4012, <https://doi.org/10.1016/j.rinp.2017.10.015>.
- [17] N. Iqbal, H. Yasmin, B.K. Kometa, A.A. Attiya, Effects of convection on sisko fluid with peristalsis in an asymmetric channel, *Math. Comput. Appl.* 25 (3) (2020), <https://doi.org/10.3390/mca25030052>.
- [18] M. Khan, M.F. Azam, A.S. Alshomrani, On unsteady heat and mass transfer in Carreau nanofluid flow over expanding or contracting cylinder with convective surface conditions, *J. Mol. Liq.* 231 (2017) 474–484, <https://doi.org/10.1016/j.molliq.2017.02.033>.
- [19] M. Khan, T. Salahuddin, Y. Elmasry, S. Aly, F. Khan, Zero mass flux and convection boundary condition effects on Carreau–Yasuda fluid flow over a heated plate, *Radiat. Phys. Chem.* 177 (2020), 109152, <https://doi.org/10.1016/j.radphyschem.2020.109152>.
- [20] M.I. Khan, F. Alzahrani, A. Hobiny, Z. Ali, Estimation of entropy generation in Carreau–Yasuda fluid flow using chemical reaction with activation energy, *J. Mater. Res. Technol.* 9 (2020) 9951–9964, <https://doi.org/10.1016/j.jmrt.2020.05.085>.
- [21] H. Waqas, S.U. Khan, M.M. Bhatti, M. Imran, Significance of bioconvection in chemical reactive flow of magnetized Carreau–Yasuda nanofluid with thermal radiation and second-order slip, *J. Therm. Anal. Calorim.* 140 (2020) 1293–1306, <https://doi.org/10.1007/s10973-020-09462-9>.
- [22] M.I. Khan, T. Hayat, S. Afzal, M.I. Khan, A. Alsaedi, Theoretical and numerical investigation of Carreau–Yasuda fluid flow subject to soret and dufour effects, *Comput. Methods Programs Biomed.* 186 (2020), 105145, <https://doi.org/10.1016/j.cmpb.2019.105145>.
- [23] N.A. Shah, A. Wakif, E.R. El-Zahar, T. Thumma, S.-J. Yook, Heat transfers thermodynamic activity of a second-grade ternary nanofluid flow over a vertical plate with Atangana-Baleanu time-fractional integral, *Alex. Eng. J.* 61 (2022) 10045–10053, <https://doi.org/10.1016/j.aej.2022.03.048>.
- [24] J.B.J. Fourier, *Theorie Analytique De La Chaleur*, Paris, 1822.
- [25] A.S. Dogonchi, D.D. Ganji, Impact of Cattaneo–Christov heat flux on MHD nanofluid flow and heat transfer between parallel plates considering thermal radiation effect, *J. Taiwan Inst. Chem. Eng.* 80 (2017) 52–63, <https://doi.org/10.1016/j.jtice.2017.08.005>.
- [26] C.I. Christov, On frame indifferent formulation of the Maxwell Cattaneo model of finite speed heat conduction, *Mech. Res. Commun.* 36 (2009) 481–486, <https://doi.org/10.1016/j.mechrescom.2008.11.003>.
- [27] V. Tibullo, V. Zampoli, A uniqueness result for the Cattaneo–Christov heat conduction model applied to incompressible fluids, *Mech. Res. Commun.* 176 (38) (2011) 77–79, <https://doi.org/10.1016/j.mechrescom.2010.10.008>.
- [28] J.G. Oldroyd, On the formulation of rheological equations of state, *Proc. Math. Phys. Eng. Sci. P Roy Soc. A-Math. Phys.* 200 (1949) 523–541, <https://doi.org/10.1098/rspa.1950.0035>.
- [29] M. Ciarletta, B. Straughan, Uniqueness and structural stability for the Cattaneo–Christov equations, *Mech. Res. Commun.* 37 (2010) 445–447, <https://doi.org/10.1016/j.mechrescom.2010.06.002>.
- [30] B. Straughan, Thermal convection with the Cattaneo Christov model, *Int. J. Heat Mass Transf.* 53 (2010) 95–98, <https://doi.org/10.1016/j.ijheatmasstransfer.2009.10.001>.
- [31] O.U. Mehmood, A.A. Qureshi, H. Yasmin, S. Uddin, Thermo-mechanical analysis of non Newtonian peristaltic mechanism: modified heat flux model, *Phys. A: Stat. Mech. Appl.* 550 (2020), 124014, <https://doi.org/10.1016/j.physa.2019.124014>.

- [32] S. Han, L. Zheng, C. Li, X. Zhang, Coupled flow and heat transfer in viscoelastic fluid with Cattaneo–Christov heat flux model, *Appl. Math. Lett.* 38 (2014) 87–93, <https://doi.org/10.1016/j.aml.2014.07.013>.
- [33] T. Hayat, M.I. Khan, M. Farooq, T. Yasmeen, A. Alsaedi, Stagnation point flow with Cattaneo–Christov heat flux and homogeneous-heterogeneous reactions, *J. Mol. Liq.* 220 (2016) 49–55, <https://doi.org/10.1016/j.molliq.2016.04.032>.
- [34] A. El Harfouf, A. Wakif, H.M. Sanaa, Analytical and numerical analysis of magneto hydrodynamic flow and heat transfer in a nanofluid via the Christov–Cattaneo heat flux theory, *Sens. Lett.* 8 (2020) 643–657, <https://doi.org/10.1166/sl.2020.4269>.
- [35] G. Rasool, A. Wakif, Numerical spectral examination of EMHD mixed convective flow of second-grade nanofluid towards a vertical Riga plate using an advanced version of the revised Buongiorno’s nanofluid model, *J. Therm. Anal. Calorim.* 143 (2021) 2379–2393, <https://doi.org/10.1007/s10973-020-09865-8>.
- [36] T. Abbas, B. Ahmad, S.U. Khan, E.U. Haq, Q.M.U. Hassan, A. Wakif, Couple stress flow of exponentially stretching sheet with Cattaneo–Christov heat flux model, *Heat Transf.* 51 (5) (2022) 4819–4832, <https://doi.org/10.1002/hjt.22531>.
- [37] A. Jamaludin, R. Nazar, I. Pop, Mixed convection stagnation-point flow of a nanofluid past a permeable stretching/shrinking sheet in the presence of thermal radiation and heat source/sink, *Energies* 12 (2019) 788, <https://doi.org/10.3390/en12050788>.
- [38] H.R. Patel, R. Singh, Thermophoresis, Brownian motion and non-linear thermal radiation effects on mixed convection MHD micropolar fluid flow due to nonlinear stretched sheet in porous medium with viscous dissipation, joule heating and convective boundary condition, *Int. Commun. Heat Mass Transf.* 107 (2019) 68–92, <https://doi.org/10.1016/j.icheatmasstransfer.2019.05.007>.
- [39] H.A. Ogunseye, P. Sibanda, H. Mondal, MHD mixed convective stagnation-point flow of Eyring–Powell nanofluid over stretching cylinder with thermal slip conditions, *J. Cent. South Univ.* 26 (2019) 1172–1183, <https://doi.org/10.1007/s11771-019-4079-6>.
- [40] B. Gebhart, L. Pera, The nature of vertical natural convection flows resulting from the combined buoyancy effects of thermal and mass diffusion, *Int. J. Heat Mass Transf.* 14 (1971) 2025–2050, [https://doi.org/10.1016/0017-9310\(71\)90026-3](https://doi.org/10.1016/0017-9310(71)90026-3).
- [41] S. Hussain, M.A. Hossain, M. Wilson, Natural convection flow from a permeable vertical flat plate with variable surface temperature and species concentration, *Eng. Comput.* 17 (2000) 789–812, <https://doi.org/10.1108/02644400010352261>.
- [42] N.C. Roy, M.A. Hossain, Numerical solution of a steady natural convection flow from a vertical plate with the combined effects of streamwise temperature and species concentration variations, *Heat Mass Transf.* 46 (2010) 509–522, <https://doi.org/10.1007/s00231-010-0591-9>.
- [43] T. Hayat, H. Yasmin, B. Ahmad, G. Chen, Exact solution for peristaltic transport of a micropolar fluid in a channel with convective boundary conditions and heat source/sink, *Z Naturforsch A* 69 (2014) 425–432, <https://doi.org/10.5560/zna.2014-0038>.
- [44] M.J. Martin, I.D. Boyd, Momentum and heat transfer in laminar boundary layer with slip flow, *J. Thermophys. Heat Trans.* 20 (2006) 710–719, <https://doi.org/10.2514/1.22968>.
- [45] K. Bhattacharyya, S. Mukhopadhyay, G.C. Layek, Similarity solution of mixed convective boundary layer slip flow over a vertical plate, *Ain Shams Eng. J.* 4 (2013) 299–305, <https://doi.org/10.1016/j.asej.2012.09.003>.
- [46] K. Cao, J. Baker, Slip effects on mixed convective flow and heat transfer from a vertical plate, *Int. J. Heat Mass Transf.* 52 (2009) 3829–3841, <https://doi.org/10.1016/j.jheatmasstransfer.2009.02.013>.
- [47] S.D. Harris, D.B. Ingham, I. Pop, Mixed convection boundary-layer flow near the stagnation point on a vertical surface in a porous medium: brinkman model with slip, *Transp. Porous Media* 77 (2009) 267–285, <https://doi.org/10.1007/s11242-008-9309-6>.
- [48] T. Hayat, H. Yasmin, A. Alsaedi, Convective heat transfer analysis for peristaltic flow of power-law fluid in a channel, *J. Braz. Soc. Mech. Sci. Eng.* 37 (2015) 463–477, <https://doi.org/10.1007/s40430-014-0177-4>.
- [49] U. Nazir, N.H. Abu-Hamdeh, M. Nawaz, S.O. Alharbi, W. Khan, Numerical study of thermal and mass enhancement in the flow of Carreau–Yasuda fluid with hybrid nanoparticles, *Case Study, Therm. Eng.* 27 (2021), 101256, <https://doi.org/10.1016/j.csite.2021.101256>.
- [50] J. Li, L. Zheng, L. Liu, MHD viscoelastic flow and heat transfer over a vertical stretching sheet with Cattaneo–Christov heat flux effects, *J. Mol. Liq.* 221 (2016) 19–25, <https://doi.org/10.1016/j.molliq.2016.05.051>.
- [51] M.I. Khan, F. Alzahrani, A. Hobiny, Z. Ali, Estimation of entropy optimization in Darcy–Forchheimer flow of Carreau–Yasuda fluid (non-Newtonian) with first order velocity slip, *Alex. Eng. J.* 59 (2020) 3953–3962, <https://doi.org/10.1016/j.aej.2020.06.057>.
- [52] L.F. Shampine, I. Gladwell, S. Thompson, *Solving ODEs With MATLAB*, Cambridge University Press, 2003.
- [53] S. Rajput, A.K. Verma, K. Bhattacharyya, A.J. Chamkha, Unsteady nonlinear mixed convective flow of nanofluid over a wedge: buongiorno model, *Waves Random Complex Media* (2021), <https://doi.org/10.1080/17455030.2021.1987586>.
- [54] R.A. Granger, *Fluid Mechanics*, Dover, New York, NY, USA, 1995.